

## Zn K-edge XANES in nanocrystalline ZnO

A Kuzmin<sup>1</sup>, S Larcheri<sup>2</sup> and F Rocca<sup>2</sup>

<sup>1</sup>Institute of Solid State Physics, University of Latvia, Riga, Latvia

<sup>2</sup>IFN-CNR, Istituto di Fotonica e Nanotecnologie del Consiglio Nazionale delle Ricerche, Sezione di Trento, Povo (Trento), Italy

E-mail: [a.kuzmin@cfi.lu.lv](mailto:a.kuzmin@cfi.lu.lv)

**Abstract.** Zn K-edge XANES in ZnO has been calculated within the full-multiple-scattering (FMS) and finite difference method (FDM) formalism using the ab initio FDMNES code. The influence of non-muffin-tin potential, bulk defects, surface termination and polarization effects on XANES has been analysed. The obtained theoretical results are compared with available experimental data for polycrystalline and nanocrystalline zinc oxide systems.

### 1. Introduction

Nanocrystalline zinc oxide (ZnO) is important technological material that finds practical applications in short-wavelength light-emitting devices, transparent conductive coatings, surface acoustic wave devices and gas sensors [1,2]. A range of methods was elaborated during last years to produce ZnO-based nano-structures by different preparation routes. A wide spread of possible ZnO nano-structures can be obtained today that requires their characterization by structural techniques such as diffraction and x-ray absorption spectroscopy (XAS).

A special role played by XAS is provoked by its local atomic and electronic structure sensitivity as well as possibility to use a number of detection methods (as transmission, fluorescence, x-ray excited optical luminescence (XEOL), total electron yield (TEY), diffraction anomalous fine structure (DAFS), etc.), being sensitive to different response channels and aspects of the structure. To extract structural information, the experimentally obtained x-ray absorption coefficient should be analyzed by sophisticated theoretical treatment procedures.

In this work, we present original results of ab initio x-ray absorption spectra (XANES) calculations of the Zn K-edge in ZnO. The influence of bulk defects, surface and polarization effects on XANES is discussed in attempt to explain few currently available experimental data [3-6].

### 2. Theoretical modelling

Hexagonal wurtzite ZnO structure (space group  $C6mc$ ), existing below 9 GPa [7], with the lattice parameters  $a=3.2495 \text{ \AA}$ ,  $c=5.2069 \text{ \AA}$  and  $u=0.345$  was used in all calculations. It can be described as a number of alternating planes composed of tetrahedrally coordinated  $O^{2-}$  and  $Zn^{2+}$  ions, stacked alternately along the  $c$ -axis. The tetrahedral coordination in ZnO results in noncentral symmetric structure and consequently piezoelectricity and pyroelectricity. The anisotropy of the ZnO structure is important for nanostructures growth and also contributes into the orientation/polarization dependence of the XANES, observed experimentally in [3,4].

The Zn K-edge XANES calculations were performed by the FDMNES code [8] in dipolar approximation within the full-multiple-scattering (FMS) and finite difference method (FDM) [9] approaches with the real energy-dependent exchange Hedin-Lundqvist potential. The two methods differ in the cluster potential construction procedure: the FMS approach utilizes the spherical muffin-tin (MT) approximation, whereas a non-muffin-tin (NMT) numerical potential, set on an equally spaced 3D-grid with a period 0.25 Å, is used in the FDM method. Note that a non-self-consistent potential is used in the FDMNES code, however we have checked that this limitation does not influence the obtained results. The FMS calculations were performed using the MT-potential constructed from 10% overlapped MT-spheres of the radii:  $R_{\text{MT}}(\text{Zn}^*)=1.18$  Å for central absorbing atom,  $R_{\text{MT}}(\text{Zn})=1.08$  Å and  $R_{\text{MT}}(\text{O})=0.95$  Å for neighbouring atoms. No broadening, except due to the core-hole, was included in all XANES calculations to outline the details of the fine structure. The final excited state was approximated by a fully relaxed configuration with a core hole at the  $1s(\text{Zn})$  level and an additional electron in the  $4p(\text{Zn})$  level.

### 3. Results and Discussion

#### 3.1. Muffin-tin versus non-muffin-tin approach.

One can expect that when the electrons distribution in a compound is not spherically symmetric, the NMT correction could become important. Therefore, the open structures or compounds with highly directional bonds are expected to be more sensible to the NMT effect than closed packed structures or compounds with ionic bonding. One can also expect that the NMT effect reduces for outer shells, especially in disordered systems, where overlap between neighbouring shells leads to the smearing of potential details. Since atomic structure of ZnO is anisotropic, it is interesting to see if the use of the NMT-potential can improve the agreement between theory and experiment.

The results for bulk ZnO obtained within MT and NMT approximations are shown in figure 1. The largest difference between two methods is observed in XANES signals calculated for small clusters. For example, the NMT XANES signal has more pronounced first peak at 6 eV after the edge for the smallest cluster, having the radius  $R=3.0$  Å and composed of only 4 oxygen atoms around central zinc atom. For increasing cluster size, the difference between the results of the MT and NMT approximations decreases. This fact is due the distribution of electron density around Zn atom is strongly anisotropic in  $\text{ZnO}_4$  tetrahedron and, thus, the NMT potential provides with presumably more precise results than the MT approximation. When the number of shells increases, the average distribution of electron density becomes more isotropic, thus reducing the difference between the results of the two methods. This means that for large ZnO clusters, the two methods should provide with close results, at least at the level of accuracy one is interested in here. Therefore, to save computation time, the MT potential approximation is used in further analysis.

Note also that the cluster having at least 5.1 Å radius (48 atoms) is required to reproduce main features of the experimental Zn K-edge XANES spectrum. Close results were obtained for bulk ZnO in [7] by the ab initio FMS FEFF8 code [10] within the MT-potential approximation.

#### 3.2. Polarization dependence.

The polarization dependence of the Zn K-edge XANES was measured experimentally in [3,4] using a sample made of the *c*-axis oriented ZnO nanorods, grown by chemical vapor deposition (CVD) method. The observed experimental XANES signals (see figures 3 in [3,4]) show strong orientation dependence especially within the first 30 eV above the edge.

Our theoretical calculations, performed for a large (8 Å) ZnO cluster, are presented in figure 2. The direction of the x-ray beam polarization was chosen along the three ZnO crystallographic axes (100), (010) and (001). As expected, the (100) and (010) orientations give similar XANES signals, which differ significantly from that for the (001) orientation. Thus, our results confirm findings of [3,4] and are able to explain variations of all features present in the experimental spectra. Besides, our results indicate that polarization effect strongly influences the amplitude of the main peak at 6 eV: since in-

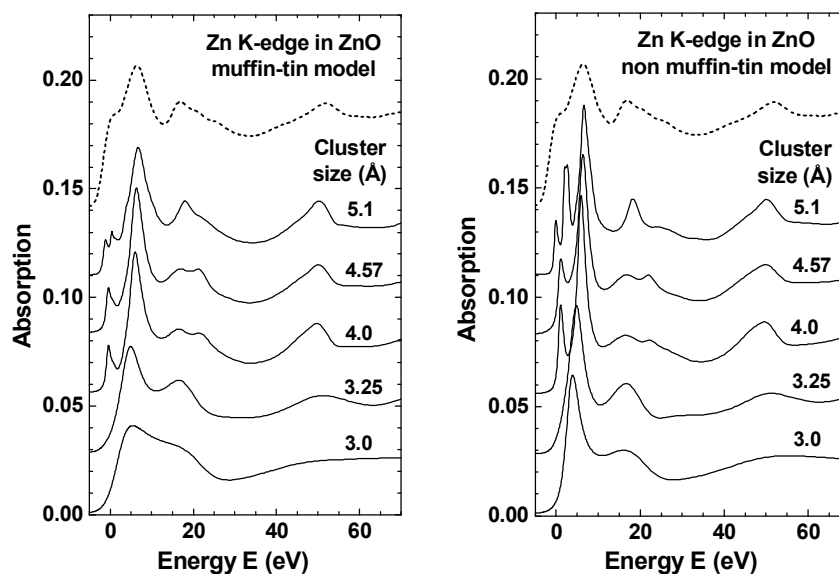
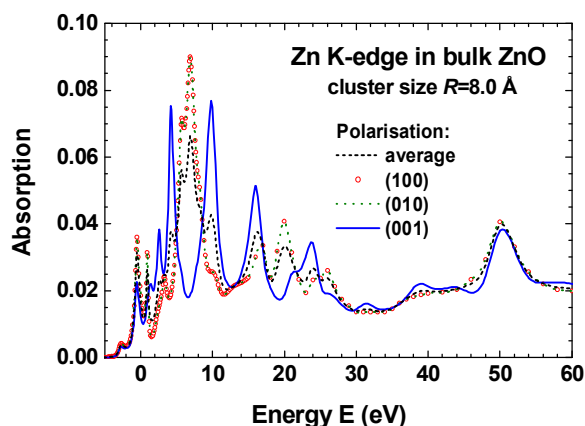


Figure 1 Zn K-edge XANES in bulk ZnO calculated by FDMNES code within the muffin-tin and non-muffin-tin approximations for clusters having different size (radius) and centred at Zn ion. The experimental XANES signal for bulk ZnO, taken from [6], is shown by dashed line. The energy origin is defined relative to the theoretical Fermi's level.



**Figure 2** (Colour online) Polarization dependence of Zn K-edge XANES in ZnO, calculated for the cluster of 8 Å radius. Dashed (black) line corresponds to the average polarization of the x-ray beam; (red) circles and dotted (green) line – to the polarization parallel to the *a* or *b* crystallographic axis, respectively; solid (blue) line – to the polarization parallel to the *c*-axis.

plane and out-of-plane orientations produce XANES signals in opposite phase. Therefore, the orientation sensitivity of Zn K-edge XANES can be among possible explanations of the differences between several nanostructured ZnO samples, observed using XEOL detection in [6].

### 3.3. Interpretation of XEOL XANES.

In our previous work [6], we have observed that in nanostructured ZnO, the Zn K-edge XEOL XANES signal, detected by measuring the intensity of the green luminescence band at 540 nm, is close to but has higher amplitude of the main peak at 6 eV (figure 1) than that measured for bulk ZnO. Note that the green luminescence of ZnO is usually associated with oxygen vacancies [11]. Therefore, to interpret the observed behaviour of the XEOL XANES signals [6], we have simulated several possible atomic environments of zinc ions in the bulk and at the surface of ZnO crystallites.

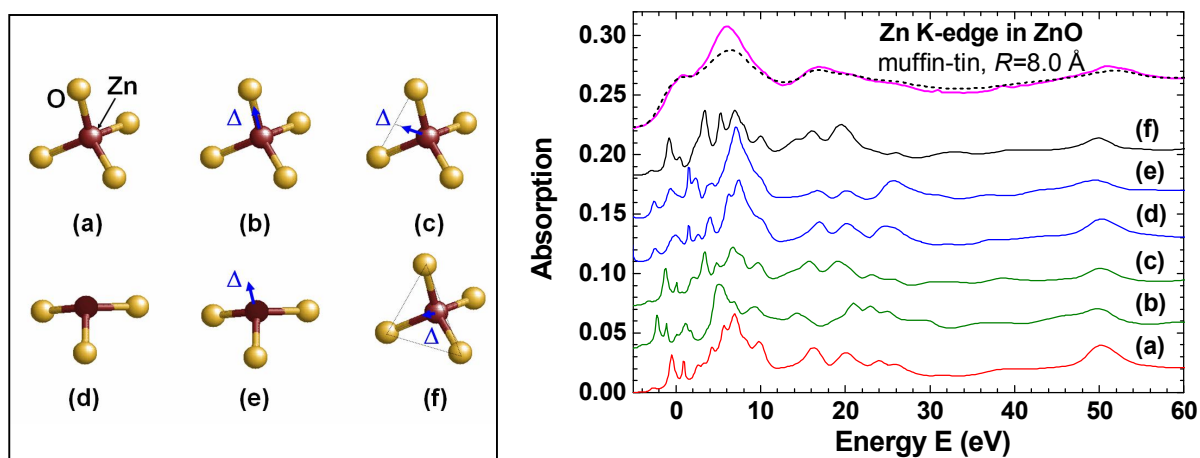


Figure 3 (Colour online) Left panel: a set of small  $[\text{ZnO}_x]$  ( $x=3, 4$ ) clusters embedded into bulk ZnO structure and used in the Zn K-edge XANES calculations by FDMNES code within the muffin-tin approximation to check the influence of Zn off-centre displacement ( $\Delta=0.3 \text{ \AA}$ ) and the presence of oxygen vacancy on the XANES signal. Right panel: the Zn K-edge XANES signals for each model. The upper two experimental XANES signals are taken from [6] and correspond to the bulk (dashed line) and thin film (solid line) zinc oxides. An increase of the peak at 6 eV intensity is well visible.

First, we will consider several bulk models (figure 3 (left panel)), which account for possible off-centre displacements of Zn ion from the centre of tetrahedron in the direction of vertex (b), edge (c) or face (f) and for the presence of oxygen vacancy, models (d) and (e), in the first shell of Zn ion. The calculated Zn K-edge XANES signals for these models are shown in figure 3 (right panel). Note that the model (a) corresponds to the zinc environment in the undistorted bulk ZnO structure.

The obtained results (figure 3 (right panel)) indicate that the off-centre displacement of Zn ion, models (b), (c) and (f), leads to a splitting of the main peak at 6 eV and, thus, cannot produce an increase of its amplitude, observed experimentally. In the model (e), the amplitude of the main peak remains unchanged, but a redistribution of the fine structure in the region 10-30 eV contradicts to the experiment (see two experimental XANES signals in figure 2 (right panel)). Therefore, the model (d) is the only one, which is able to account for a small increase of the main peak, leaving roughly unchanged other peaks. However, one should note that the calculated increase of the main peak amplitude for model (d) is rather small compared to the one observed experimentally.

The nanostructured ZnO has a large surface-to-bulk ratio, therefore one can expect that the XANES signal can have some surface sensitivity. Further, we will consider two types of surfaces (figure 4): the polar (0001) surface perpendicular to the  $c$ -axis and the (1000) surface perpendicular to the  $a$ -axis. Depending on the surface coverage with oxygen atoms, three situations were analyzed: (i) oxygen terminated surface, i.e. zinc atoms in the uppermost layer are coordinated with 4 oxygen atoms; (ii) oxygen non-terminated surface, i.e. zinc atoms in the uppermost layer are coordinated with only 3 oxygen atoms; (iii) one-oxygen terminated surface, i.e. only absorbing zinc atom located in the uppermost layer has 4-fold coordination, whereas other zinc atoms are 3-fold coordinated. The absorber Zn atom was always located in the top surface layer, and the ZnO crystal in the direction opposite to the surface was considered to be infinite and having the bulk structure. Such model, while being a crude approximation of real situation, allows however to estimate the effect of surface termination.

The calculated Zn K-edge XANES signals for three situations are shown in figure 5 by dashed, dotted and dash-dotted lines, respectively, in comparison with the bulk signal. The important result is that the amplitude of the main peak at 6 eV increases significantly for both surfaces when they are terminated with oxygen atoms. Moreover, the oxygen terminated (0001) surface gives the XANES signal, having the main peak being slightly higher than in the bulk case. This fact provides with

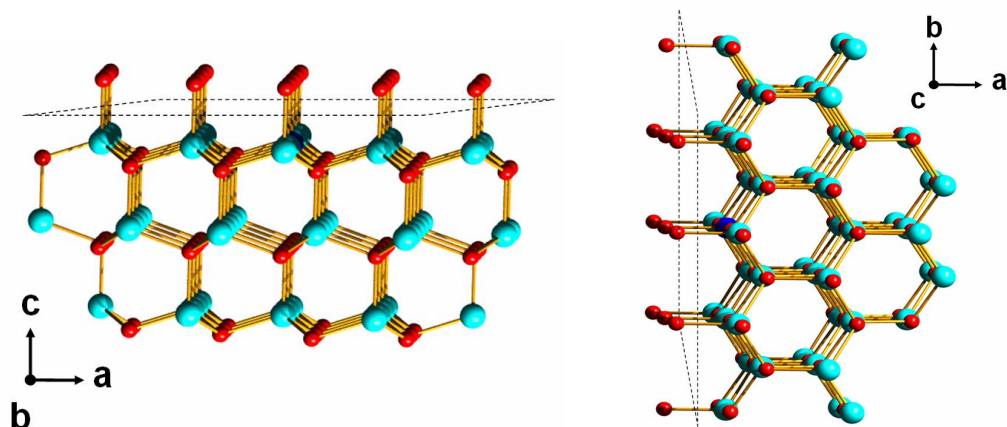


Figure 4 (Colour online) Left panel: oxygen terminated polar ZnO(0001) surface. Right panel: oxygen terminated ZnO(1000) surface. Small (red) balls are oxygen atoms; large (cyan) balls – zinc atoms.

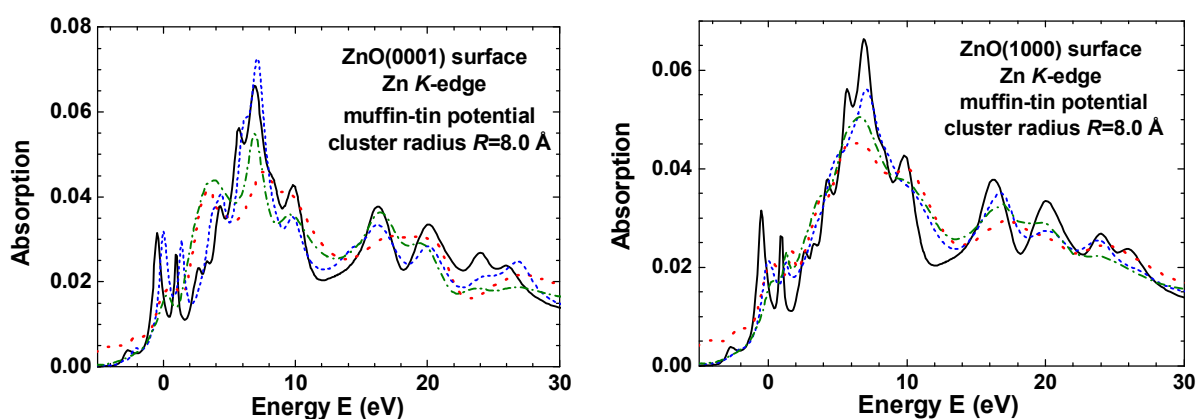


Figure 5 (Colour online) Left panel: oxygen terminated polar ZnO(0001) surface. Right panel: oxygen terminated ZnO(1000) surface. Solid (black) line is bulk ZnO; dashed (blue) line – oxygen terminated surface; dash-dotted (green) line – one-oxygen terminated surface; dotted (red) line – oxygen non-terminated surface.

another possible model for explaining an increase of the XEOL XANES in nanostructured ZnO by the presence of defect luminescence centres close to the oxygen terminated surface.

#### 4. Conclusions

Zn K-edge XANES in ZnO was calculated using the ab initio FDMNES code and the obtained results were compared with available [3-6] experimental data. The effects of non-muffin-tin potential correction, cluster size, bulk defects, surface termination and polarization on the shape of the XANES signal were addressed with particular emphases on the variation of the main peak (at about 6 eV above the absorption edge) amplitude. The obtained results allow to withdraw the following conclusions.

The non-muffin-tin correction was found to be important in the case of anisotropic structures, however, it is not crucial for large cluster sizes in 3D-periodic systems as ZnO crystal due to that the progressive overlap between outer shells smears the effect of the anisotropy of the first shell  $[ZnO_4]$  tetrahedron.

The theoretical calculations are able to reproduce qualitatively the experimental XANES signals from bulk ZnO and the polarization dependence [3,4] of the experimental spectra in oriented ZnO

films. The Zn K-edge XANES signal was found to be also sensitive to the presence of oxygen vacancies and a type of surface sites.

Finally, the increase of the amplitude of the main peak, observed in Zn K-edge XEOL XANES spectra of nanostructured ZnO films [6], can be due to the partial influence of polarization effect, the contribution from the oxygen terminated surfaces or the presence of oxygen vacancies in the first coordination shell of zinc in the bulk. Note that a change of this peak was also observed in the reference [5], devoted to ZnO nanorods of different diameters (d): the peak amplitude increases for nanorods with smaller diameter.

### Acknowledgments

This work was partially supported by the European Commission through the FP6 STREP Project "X-TIP" (Contract No. NMP4-CT-2003-505634) and Latvian Government Research Grant No. 05.1717. The authors are grateful to Dr. O. Šipr for many useful discussions.

### References

- [1] Özgür Ü, Alivov Ya I, Liu C, Teke A, Reshchikov M A, Doğan S, Avrutin V, Cho S J and Morkoç H 2005 *J. Appl. Phys.* **98** 041301
- [2] Wang Z L 2004 *Materials Today* **7** 24
- [3] Lee E Y M, Tran N, Russell J, Lamb R N 2002 *J. Appl. Phys.* **92** 2996
- [4] Chiou J W, Mookerjee S, Rao K V R, Jan J C, Tsai H M, Asokan K, Pong W F, Chien F Z, Tsai M H, Chang Y K, Chen Y Y, Lee J F, Lee C C and Chi G C 2004 *Appl. Phys. Lett.* **84** 3462
- [5] Chiou J W, Krishna Kumar K P, Jan J C, Tsai H M, Bao C W, Pong W F, Chien F Z, Tsai M H, Hong I H, Klauser R, Lee J F, Wu J J and Liu S C 2004 *Appl. Phys. Lett.* **85** 3220
- [6] Larcheri S, Armellini C, Rocca F, Kuzmin A, Kalendarev R, Dalba G, Graziola R, Purans J, Pailharey D and Jandard F 2006 *Superlattices and Microstructures* **39** 267
- [7] Decremps F, Datchi F, Saitta A M, Polian A, Pascarelli S, Di Cicco A, Itié J P and Baudelet F 2003 *Phys. Rev. B* **68** 104101
- [8] Joly Y 2001 *Phys. Rev. B* **63** 125120
- [9] Kimball G E and Shortley G H 1934 *Phys. Rev.* **45** 815
- [10] Ankudinov A L, Ravel B, Rehr J J and Conradson S D 1998 *Phys. Rev. B* **58** 7565
- [11] Wu X L, Siu G G, Fu C L and Ong H C 2001 *Appl. Phys. Lett.* **78** 2285